Molecular Docking and Molecular Dynamics Simulations of Molnupiravir Against Covid-19

Tugce Sinem OKTEMER[1]✎, Zeynep C. ONEM[2], Sefa ÇELİK[2], Aysen OZEL[2], Sevim AKYUZ[3]

[1] Institute of Graduate Studies in Sciences, Istanbul University, Istanbul, Turkey
[2] Physics Department, Science Faculty, Istanbul University, Istanbul, Turkey
[3] Physics Department, Science and Letters Faculty, Istanbul Kultur University, Istanbul, Turkey

✉: scelik@istanbul.edu.tr iD [1] 0009-0001-9059-1216   iD [2] 0000-0001-6216-1297   iD [3] 0000-0001-6216-1297
iD [4] 0000-0002-8680-8830   iD [5] 0000-0003-3313-6927

ABSTRACT

The most stable conformation of molnupiravir ($C_{13}H_{19}N_3O_7$), which is frequently used in the COVID-19 treatment, was elucidated by the Spartan06 program. Using the CAVER program, the potential active binding sites that belong to the spike glycoprotein, ACE2 receptor, and both the apo and holo forms of the main protease enzyme(M^{pro}) of COVID-19 were identified. To determine the binding affinity of molnupiravir to target receptors, molecular docking analyses were carried out using Autodock Vina. The results of molecular docking calculations of the molnupiravir with the spike glycoprotein (PDB ID:6VXX), ACE2 (PDB ID:6M0J;1R42), the apo form (PDB ID: 6M03) and the holo form of COVID-19 M^{pro} (PDB ID: 6LU7) showed strong binding affinities at -7.8, -7.7, -7.7, -7.1, and -7.4 kcal/mol, respectively. Moreover, top-scoring ligand-receptor complex of the molnupiravir with ACE2 (1R42) were subjected to 50 ns all-atom MD simulations to investigate the ligand-receptor interactions in more detail.

Keywords: ACE2, Molecular docking, Molecular dynamics, Molnupiravir, Spike glycoprotein

Molnupiravir'in Covid-19'a Karşı Moleküler Kenetlenme ve Moleküler Dinamik Simülasyonları

ÖZ

COVID-19 tedavisinde kullanılan molnupiravir'in ($C_{13}H_{19}N_3O_7$) en kararlı konformasyonu Spartan06 programı ile belirlenmiştir. CAVER programı kullanılarak, spike glikoprotein, ACE2 reseptörü ve COVID-19'un ana proteaz enziminin (Mpro) apo ve holo formlarına ait potansiyel aktif bağlanma bölgeleri tanımlanmıştır. Molnupiravir'in hedef reseptörlere bağlanma afinitesini belirlemek için Autodock Vina kullanılarak moleküler kenetlenme analizleri gerçekleştirilmiştir. Molnupiravir'in spike glikoprotein (PDB ID: 6VXX), ACE2 (PDB ID: 6M0J; 1R42), apo formu (PDB ID: 6M03) ve COVID-19 M^pro'nun holo formu (PDB ID: 6LU7) ile moleküler kenetlenme hesaplamalarının sonuçları sırasıyla -7,8, -7,7, -7,7, -7,1 ve -7,4 kcal/mol'de güçlü bağlanma afinitesi göstermiştir. Ayrıca, ligand-reseptör etkileşimlerini daha detaylı incelemek amacıyla molnupiravirin ACE2 (1R42) ile en yüksek skor alan ligand-reseptör kompleksinin 50 ns MD simülasyonu yapılmıştır.

Anahtar Kelimeler: ACE2, Moleküler kenetlenme, Moleküler dinamik, Molnupiravir, Spike glikoprotein

INTRODUCTION

Severe acute respiratory syndrome coronavirus 2 (SARS-CoV-2), a coronavirus variant that belongs to the family of Coronaviridae, is one of the seven coronaviruses known to infect humans. Severe acute respiratory syndrome coronavirus (SARS-CoV) and middle east respiratory syndrome coronavirus (MERS-CoV) can also be given as examples for coronaviruses that can infect humans [1]. Coronaviruses are single-stranded positive RNA viruses that have the biggest known RNA virus genomes [2]. SARS-CoV-2, which is an RNA virus, is

the reason behind the COVID-19 pandemic [3]. Although effective vaccines are available for the rapidly spreading COVID-19 pandemic, it is necessary to develop antiviral drugs that can be used against COVID-19 [3,4]. Molnupiravir is among the drugs that could be of use for the therapy of COVID-19 patients. The fact that molnupiravir does not require a hospital environment to be used by patients and its easy transportation is a significant difference between molnupiravir and other COVID-19 drugs [5]. Molnupiravir is an oral antiviral prodrug of ribonucleoside analogue β-D-N4-hydroxycytidine and this drug gets activated by

metabolism after entering the body [5,6]. Studies have shown that molnupiravir, which was discovered for the treatment of Venezuelan equine encephalitis virus (VEEV) and developed for the treatment of influenza, has the potential to treat diseases caused by RNA viruses [7]. Preclinical studies have revealed that molnupiravir has a broad-spectrum antiviral activity against all coronavirus types, such as SARS-CoV-2, and clinical trials for the drug's usage in the COVID-19 treatment reached the final stage [5,8]. The US Food and Drug Administration issued molnupiravir an Emergency Use Authorization for non-hospitalized adult COVID-19 patients recently [9].

Up until this point, many studies have shown the effect of molnupiravir on COVID-19 and its usability to treat coronavirus. It was observed that molnupiravir showed efficacy against SARS-CoV-2 in vitro when it was examined in a human airway epithelial cell culture system representing human airway epithelial cells [10]. In animal experiments, mice infected with SARS-CoV-2 were treated with molnupiravir. Molnupiravir treatment slowed down the rate of SARS-CoV, SARS-CoV-2 and MERS-CoV virus replication in mice and it improved the respiratory functions of the mice and reduced body weight losses [8,10]. While the molnupiravir effect on virus replication in mice could be observed, the effect of molnupiravir on the rate of transmission of the virus could not be observed because virus transmission to uninfected mice is not possible [6,8]. The effectiveness of molnupiravir in preventing the transmission of SARS-CoV-2 has been investigated through studies on ferrets. This is possible because ferrets can effectively spread the virus in a similar way to young adult humans [6]. As a result of the molnupiravir treatment of ferrets, it was observed that SARS-CoV-2 transmission to untreated animals could be prevented entirely [6]. This study showed that molnupiravir can be effective in stopping disease spread in the community and that secondary spread of SARS-CoV-2 can possibly be prevented with early treatment [6,8]. Positive results were also acquired in phase 1, phase 2 and phase 3 studies with humans [5]. Studies have shown that molnupiravir can be an effective antiviral drug that can be used for the COVID-19 treatment. In this study, the interaction of molnupiravir molecule with the apo and holo form of the main protease enzyme (M^{pro}) of COVID-19, the spike glycoprotein, ACE2 and dACE2 proteins were examined by molecular docking analysis and their binding affinities were found. The main protease enzyme, M^{pro}, plays a crucial role in virus replication and maturation [3]. This is why it has become one of the most critical target proteins for antiviral drug discovery and treatments for SARS-CoV-2 [2]. Since no known human protease shows the cleavage property of M^{pro}, a drug specially developed for M^{pro} will possibly have few side effects on humans [3]. The main protease M^{pro} has two different conformational forms; these are the holo form and the apo form [11]. In this study, molecular docking analysis was performed for both forms of M^{pro}. Another essential protein examined in this study is the spike glycoprotein. The spike

glycoprotein (S protein) is the first section to come into contact with the host cells since it is located on the surface of the virus [1,12]. The spike glycoprotein's role in binding the virus to host cells by receptors and entering the cell is significant. Different types of coronaviruses can enter the cell using different cell receptors [1]. SARS-CoV-2 enters the host cells through angiotensin converting enzyme 2 (ACE2), which is a cell receptor [12]. For the virus to be able to infiltrate into the human cell, spike glycoprotein must bind with ACE2 [1,12]. For this reason, both have been one of the main targets of vaccines and drugs produced.

Studies have shown that the apo and holo forms of the main protease enzyme (M^{pro}) of COVID-19, spike glycoprotein and ACE2 proteins are important targets for drugs produced for COVID-19 treatment, so for molnupiravir to work against COVID-19, it must be able to bind to these proteins. For this reason, firstly, the most stable conformer of the molnupiravir molecule was found by using conformation analysis. Then we performed molecular docking analysis to determine the binding affinities of molnupiravir molecule and the apo form and holo form of COVID-19 main protease enzyme (M^{pro}), the spike glycoprotein, and ACE2 proteins.

METHODS and CALCULATIONS

The most stable conformer of the investigated molecule was ascertained by evaluating all the possible conformations with the Spartan06 software [13] and the AM1 model, which is a semi-empirical quantum mechanical approach [14].

The CAVER software [15] was used to determine the active sites on the receptor's surface. Molecular docking simulations were executed on the identified active sites via AutoDock-Vina [16]. The binding free energies of the most stable ligand-receptor were calculated by a computer-aided, fragment-based drug discovery web server, known as the ACFIS (ACFIS 2.0) [17-20].

Through the application of the Groningen Machine for Chemical Simulations (GROMACS) software package [21-25] along with the GROMOS96 43a1 force field [26-32], a molecular dynamics (MD) simulation was done on the ligand-receptor complex formed by molnupiravir and the ACE2 enzym (1R42). Molnupiravir-protein complex that exhibited the lowest binding energy was chosen for molecular dynamics (MD) simulation. The SPC water model was performed in a triclinic periodic box for the solvation of the complex. 0.15 M of NaCl was incorporated after neutralizing the system. Utilizing the steepest descent method, the minimization process of energy was carried out for the duration of 50,000 steps. The MD simulation was performed at a constant temperature of 300 K with constant volume, constant amount of atoms (NVT), and under an invariant pressure of 1.0 bar (NPT) according to the GROMACS equilibration parameters. The Leap-frog molecular dynamics integrator was applied then, establishing an approximate number of simulation frames at 1000. In order to verify the ligand-enzyme complex's

stability, the MD simulation was set to operate for 50 ns. The root mean square deviation (RMSD), root mean square fluctuations (RMSF), the radius of gyration (Rg), protein-ligand hydrogen bonding and Solvent Accessible Surface Area (SASA) were determined with MD simulation to analyze the trajectories of the simulation.

RESULTS

The most stable conformer of Molnupiravir, obtained from the findings of the conformational analysis, is illustrated in figure 1.
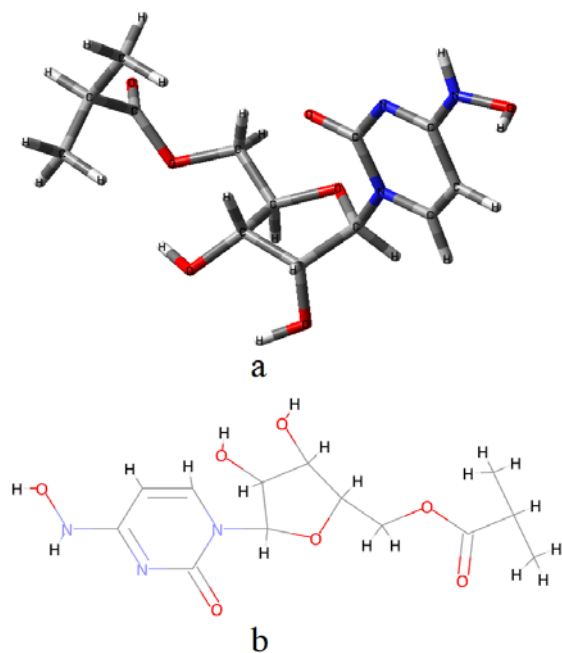
Figure 1. The molecular structure obtained from the conformational analysis of the most stable conformer (a) and 2D representation (b) of Molnupiravir

Molecular Docking

Spike glycoprotein (PDB ID: 6VXX), ACE2 (PDB ID: 6M0J; 1R42), the apo form of COVID-19 M^{pro} (PDB ID: 6M03) and the holo form of COVID-19 M^{pro} (PDB ID: 6LU7)'s crystal structures were taken from the protein databank [33-37]. Molecular docking calculations were done after the removal of water and the addition of polar hydrogens to the receptors. In addition to that, grid size of 40 Å × 40 Å × 40 Å was used.

The interactions present between the drug and the proteins used in this study are shown in Figures 2-6 and Table 1.

Based on the molecular docking results between Molnupiravir and ACE2 (PDB ID: 6M0J) (Figure 2), several interactions between the ligand and receptor were detected, including a hydrogen bond with Lys187 at a bond length of 2.61 Å, a pi-sigma interaction with Tyr202 at 3.75 Å, hydrogen bonds with Trp203 at 2.05 Å and 2.19 Å bond lengths, a carbon hydrogen bond with Asp206 at 3.61 Å, as well as hydrogen bonds with

Asp509, Ser511, and Arg514 at bond lengths of 2.08 Å, 2.18 Å, and 2.55 Å, respectively.
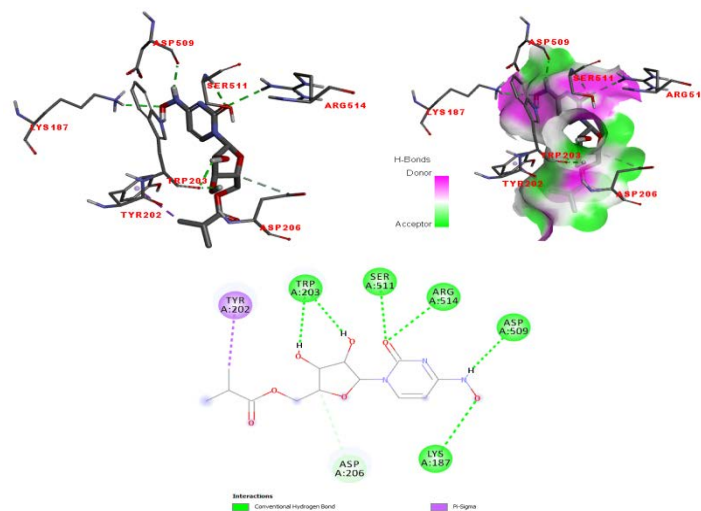
Figure 2. The three-dimensional docked views representing the most stable conformer of Molnupiravir interacting with the ACE2 (PDB ID: 6M0J). The interaction diagrams of the ligand are shown (binding affinity, -7.7 kcal/mol; binding energy -13.14 kcal/mol)

The interactions between Molnupiravir and COVID-19 M^{pro} (Apo form) (Figure 3) were found to include a hydrogen bond with His41 at a bond length of 2.22 Å, a hydrogen bond with Phe140 at 1.98 Å, a hydrogen bond with Asn142 at 2.81 Å, hydrogen bonds with Cys145 at 3.6 Å and 3.74 Å, and a hydrogen bond with His163 at 2.31 Å. Additionally, a hydrogen bond was observed at 2.92 Å, a pi-anion interaction at 4.7 Å, and an unfavorable donor-donor interaction at 2.46 Å with Glu166. Finally, a hydrogen bond with Gln189 was identified at a bond length of 1.86 Å.
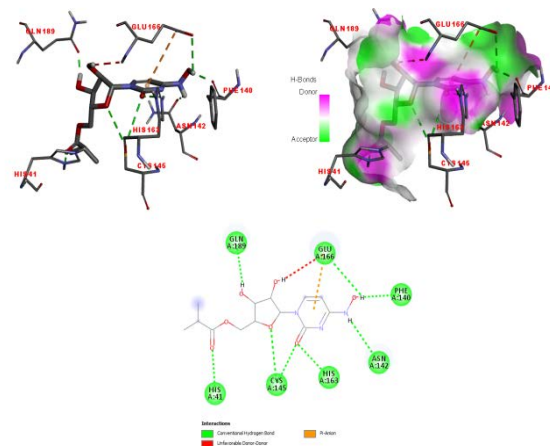
Figure 3. The three-dimensional docked views showing the most stable conformer of molnupiravir interacting with the Apo form of M^{pro} (PDB ID: 6M03). The ligand interaction diagrams belonging to the receptor-ligand

complexes are illustrated (binding affinity, -7.1 kcal/mol; binding energy -17.38 kcal/mol)

Through the molecular docking analysis between Molnupiravir and COVID-19 M^pro (Holo form) (Figure 4) the interactions between the ligand and receptor were revealed. A pi-sigma interaction was observed with His41 at a bond length of 3.96 Å. Furthermore, a hydrogen bond was formed with Leu141 at a bond length of 2.07 Å, and another hydrogen bond was detected at a 2.14 Å bond length with Gly143. An unfavorable donor-donor interaction with Ser144 was obtained at a bond length of 1.46 Å, along with a hydrogen bond at 2.58 Å. In addition, a hydrogen bond was present with Cys145 at a bond distance of 2.11 Å, as well as a pi-alkyl interaction at 5.11 Å. Two hydrogen bonds were also detected, one at a bond length of 2.28 Å with His163, and another at 1.88 Å with Glu166.
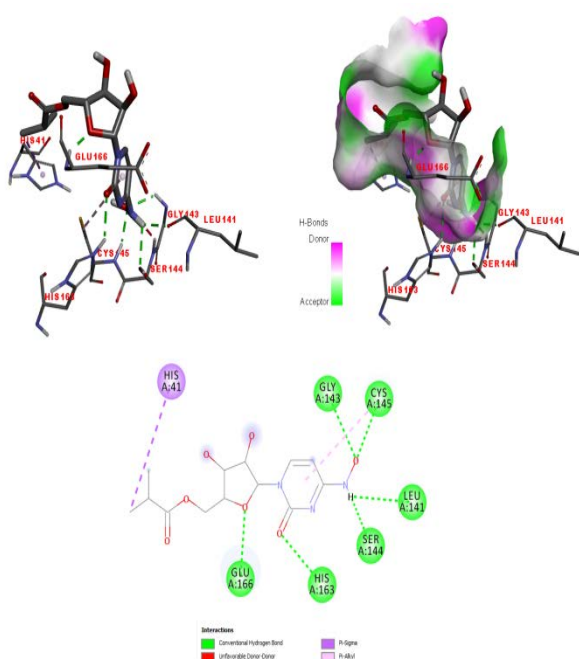
Figure 4. The three-dimensional docked views that represent the most stable conformer of molnupiravir interacting with the Holo form of M^pro (PDB ID: 6LU7). The interaction diagrams of the ligand are illustrated (binding affinity, -7.4 kcal/mol; binding energy -22.56 kcal/mol)

The molecular docking analysis revealed various interactions between Molnupiravir and Spike glycoprotein (Figure 5). These interactions include hydrogen bonds with Arg1091 at a bond length of 2.68 Å, and with Glu1092 at 2.02 Å, an unfavorable donor-donor interaction at a 1.51 Å bond length with Thr1105, two hydrogen bonds at 2.59 Å and 2.77 Å bond lengths with Gln1106, two more hydrogen bonds at 1.96 Å and 2.11 Å bond lengths with Glu1111. Moreover, there are hydrogen bonds observed at a bond length of 2.35 Å with Asp1118 and at a 2.15 Å bond length with Asn1119. A

pi-sigma interaction at 3.95 Å with Phe1121 was also detected.
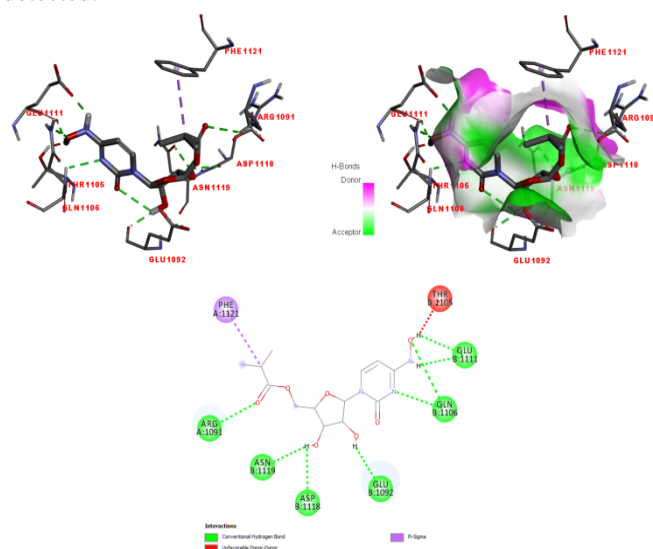
Figure 5. The three-dimensional docked views that show the most stable conformer of molnupiravir interacting with the Spike glycoprotein (PDB ID: 6VXX). The interaction diagrams of the ligand belonging to the receptor-ligand complexes are illustrated (binding affinity, -7.8 kcal/mol; binding energy -15.07 kcal/mol)

Several interactions between Molnupiravir and ACE-2 (PDB ID: 1R42) were identified (Figure 6). These interactions are composed of a carbon hydrogen bond with Gln98 at a bond length of 3.59 Å, a hydrogen bond with Gln102 at 2.41 Å, two hydrogen bonds with Tyr196 at 2.55 Å and 2.74 Å. Additionally, a hydrogen bond was observed with Gly205 at 2.83 Å and Asp206 at 2.91 Å. A hydrogen bond at 2.61 Å and an unfavorable donor-donor interaction at 2.24 Å were formed with Glu208. There is a hydrogen bond at a bond length of 2.2 Å with Asn210 and additional hydrogen bonds at 2.19, 2.34, and 2.67 Å with Lys562.
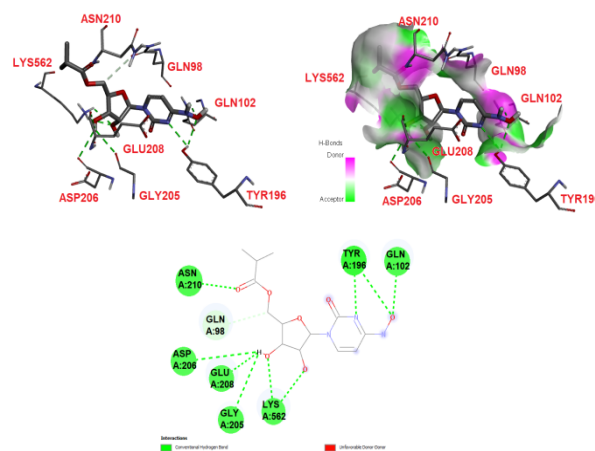
Figure 6. The three-dimensional docked views of the most stable conformation of molnupiravir interacting

with ACE2 (PDB ID: 1R42). The interaction diagrams of the ligand belonging to the receptor-ligand complexes are illustrated (binding affinity, -7.7 kcal/mol; binding energy -22.43 kcal/mol)

**Table 1**. Binding affinity and interacting residues between target protein and Molnupiravir.

| Target Protein	Binding Affinity kcal/mol	Interacting Residues	Chain Length (Å)
ACE2 (6M0J)	-7.7	Lys187	2.61
		Tyr202	3.75
		Trp203	2.05,2.19
		Asp206	3.61
		Asp509	2.08
		Ser511	2.18
		Arg514	2.55
apo-form (6M03)	-7.1	His41	2.22
		Phe140	1.98
		Asn142	2.81
		Cys145	3.6,3.74
		His163	2.31
		Glu166	2.46, 2.92, 4.7
		Gln189	1.86
Holo-form (6LU7)	-7.4	His41	3.96
		Leu141	2.07
		Gly143	2.14
		Ser144	1.46, 2.58
		Cys145	2.11, 5.11
		His163	2.28
		Glu166	1.88
Spike glycoprotein (6VXX)	-7.8	Arg1091	2.68
		Glu1092	2.02
		Thr1105	1.51
		Gln1106	2.59, 2.77
		Glu1111	1.96, 2.11
		Asp1118	2.35
		Asn1119	2.15
		Phe1121	3.95
ACE-2 (1R42)	-7.7	Gln98	3.59
		Gln102	2.41
		Tyr196	2.55, 2.74
		Gly205	2.83
		Asp206	2.91
		Glu208	2.24, 2.61
		Asn210	2.2
		Lys562	2.19, 2.34, 2.67

Molecular Dynamics

The interactions between molnupiravir and the 1R42 receptor and the binding stability were evaluated by conducting a molecular dynamics (MD) simulation. The root mean square deviation (RMSD) for the receptor and ligand, the root mean square fluctuation (RMSF) for the receptor, the radius of gyration (Rg), protein-ligand hydrogen bonding, and solvent accessible surface area (SASA) were determined by the MD trajectory analysis.

For the comparison of different atomic conformations regarding a given molecular system, the root mean square deviation (RMSD) of a ligand or a protein is applied. The RMSD is a measure of the change seen in the conformation of the ligand or protein, and if the RMSD result shows a small variation, then there are minimal conformation changes; therefore, the complexes are stable. The RMSD value deviations are more important compared to the mean value. A slight deviation in the value also means slight changes in the conformation of the structure. The accepted deviation for the RMSD plot is <4 Å for that complex to be stable enough. In this study, the RMSD analysis was applied separately to determine the displacement in the ligand and the receptor compared to their starting positions. The RMSD graph, which is shown in Figure 7(a), reveals the magnitude of structural deviation that the Ca atoms of the complexes have during the 50 ns-long MD simulations. The RMSD results, which belong to the protein backbone (PDB ID: 1R42) of the complex with molnupiravir, change between 2.21 and 4.07 Å, with an average of 3.22 Å. The RMSD graph of the ligand shown in Figure 7(b) illustrates the structural deviation for the atoms of the ligand in the complexes (1r42) during the 50 ns simulations. In the molnupiravir-1r42 complex the trajectory showed a fluctuation at the beginning but stabilized after 8 ns and appeared to remain stable until 50 ns. Structural variation has an effect over the compactness of the protein after the binding of the investigated protein to the ligand, and the radius of gyration value (Rg) reveals it. A protein that has a folded conformation has a low Rg value, while a protein with an unfolded conformation has a high Rg value. The Rg value changes after the binding of the ligand and protein and causes an alteration in the conformation of the protein. Figure 7(c) shows the Rg plots of the molnupiravir/1r42 complex. The Rg values of the protein (1r42)-molnupiravir complex were found within the range of 24.4–25.3 Å and had some small fluctuations. The RMSF gives information about the fluctuations or local modifications in the residues of a protein–ligand complex. The residues of amino acid in each complex displayed minor variations throughout the entire simulation, as seen in Figure 7(d). Hydrogen bonds are crucial in understanding the stability of the conformation since they play a role in protein-ligand binding. There have been little differences in the hydrogen bonds within the protein of the complex. The graph of the number of hydrogen bonds (HB) formed throughout the MD simulation as a function of time is shown in Figure 8(a) and six hydrogen bonds between the molnupiravir and 1r42 were revealed during 50 ns. To analyze the solvent attributable regions for each of the simulation systems, the solvent accessibility surface area (SASA) calculations were done in this study. A higher SASA profile suggests an expanded protein surface area, while a lower SASA profile suggests possible truncation of the protein complexes. The SASA graph of molnupiravir-1r42 complex is shown in Figure 8(b). The determined result of the SASA for the investigated complex is about

245 nm2. Higher values of the SASA indicate more hydrophilicity. Small changes were expected for complex structures and the SASA did not show any significant changes.
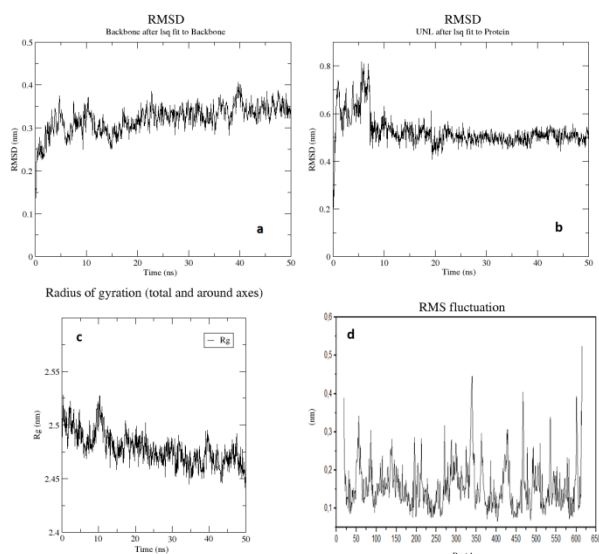
Figure 7. The final results of the simulation and the analysis of structural stability for the molnupiravir-1R42 complex. (a) The root mean square deviation (RMSD) graph of the protein, (b) the RMSD graph of the ligand, (c) the radius of gyration (Rg) graph, (d) the root mean square fluctuation (RMSF) graph.
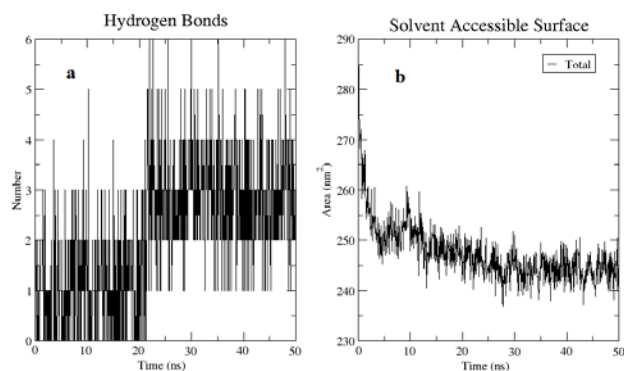
Figure 8. (a) Hydrogen bond graph, and (b) the solvent accessible surface area (SASA) graph of the molnupiravir-1R42 complex.

DISCUSSION

In a study on the docking simulations of Paritaprevir with ACE2, it was found that the ligand interacted with ACE2 residues Asn103, Gly104, Asp206 and Lys562 [38]. In another study on the docking simulations of Darunavir with ACE2, it was found that the ligand interacted with ACE2 residues Leu95, Gln102, Asn103, Asn194, Tyr196, Tyr202, Trp203, Gly205, Asp206, Tyr207, Glu208, Val209, Ala396, Lys562, Glu564, Pro565 and Trp566 [39]. The active sites of ACE2 found by our calculations are highly compatible with the conclusions

of Mahdian et al. and Rahman et al. [38,39]. In a previous research authored by Celik et al., the docking simulations of Cepharanthine with the Apo form of M^{pro} were investigated, and the results of that study have shown that the ligand interacted with residues His41, Asn142 and Cys145 of the Apo form of M^{pro}, through alkyl, pi-alkyl, pi-donor hydrogen bond interactions [40]. The active site of the Apo form found by the docking of Cepharanthine was compatible with the active site identified by the calculations of our study. In a different study, when the docking simulations of Succinic acid with the Apo form of Mpro were examined by Sagaama et al., it was observed that the ligand interacted with residues Phe140, Leu141, Asn142, Gly143, Ser144, Cys145, His163, Met165, Glu166, and His172 of the Apo form of Mpro by means of van der Waals, unfavorable donor-donor, and hydrogen bond interactions [41]. The calculations of our study was also compatible with the active site of the Apo form found by the docking of Succinic acid. The previous study in which Celik et al. investigated the docking simulations of Cepharanthine, it was shown that the ligand interacted with residues Glu166, Pro168, Gln189, and Thr190 of the Holo form of M^{pro}, via pi-alkyl, pi-anion, and carbon hydrogen bond interactions [40]. The active site revealed by the docking of Cepharanthine to the Apo form of M^{pro} demonstrated significant compatibility with the active site determined by the calculations of our study. In an investigation done by Vijayakumar et al., the docking simulations of 14-deoxy-11,12-didehydroandropholide were carried out with the Holo form of M^{pro}, and it was found that the ligand interacted with His41, Tyr54, Leu141 and Ser144 residues of the Holo form of M^{pro}, through hydrogen bond interactions [42]. The active site of the Holo form of M^{pro} identified in our study aligned well with the active site identified by of Vijayakumar et al. [42], where 14-deoxy-11,12-didehydroandropholide was docked to the Apo form of M^{pro}. The docking simulations of Sauchinone with the Spike glycoprotein were investigated by Romeo et al. in a previous study [43]. The results showed the interactions between the ligand and the Arg1091, Gly1093, and Asp1118 residues of the Spike glycoprotein, which occured through hydrogen bond interactions [43]. It was determined that Withasomnine interacted with spike glycoprotein's residues Thr912, Glu1092, Val1104, Thr1105, Gln1106, Glu1111, Gln1113 and Asn1119 in a study on the docking simulations conducted by Srivastava et al. [44]. The spike glycoprotein's active site, which is revealed by our calculations, showed high compatibility with the active sites determined by the dockings of Sauchinone [43] and Withasomnine [44]. The active site identified by the calculations of our study exhibited a high degree of compatibility with the active site found for Curcumin, Demethylcurcumin, 1-(3,4-Dihydroxyphenyl)-7-(4-Hydroxy-3-Methoxyphenyl)Hepta-1,6-diene-3, 5-Dione, (E)-Ferulic acid, Vanillic acid, Carvacrol, (E)-Carveol, E-4-(4-Hydroxy-3-Methoxyphenyl)-3-Buten-2-One, Terpinolene, Vanillin, (Z)-Ferulic Acid, Thymol and Limonene molecules investigated by a study of Khan et

al. [45]. In research using a thiazole derivative, it was observed that the TAZD8 molecule made H-pi interactions with both Ala99 and Leu391, H-donor interactions with GLN102, and cation-pi interactions with Lys562 [46]. In a different investigation by Mohan et al., the Atazanavir molecule was found to have interactions with amino acids Leu95, Arg98, Ala99, Gln102, Tyr196, Trp203, Gly205, Asp206, Glu208 and Arg219 of the target receptor [47].

CONCLUSION

Assessing the binding affinity of the active compound to target proteins that are involved in viral entry, replication, and maturation is the goal of this investigation. It also examines the modeling and simulation of the virus-induced host cell maturation in silico.The most stable conformer of molnupiravir was determined in consideration of the significance of the relationship between structure and activity in bioactive molecules. The binding mechanism of the molnupiravir with the apo- and holo- forms of M^{pro}, the spike glycoprotein and ACE2 was demonstrated in the present study. We provide detailed insights into the types of molecular interactions, such as electrostatic, hydrogen-bonding interactions, etc., that contribute to these geometric alterations. The binding affinities of the Molnupiravir molecule against the target receptors ACE2(6M0J), apo-form(6M03), holo-form(6LU7), spike glycoprotein (6VXX), and ACE-2 (1R42) were calculated to be -7.7, -7.1, -7.4, -7.8, and -7.7 kcal/mol, respectively. Thus, it was found that stable complexes were formed. Through the molecular dynamic calculation, the RMSD graph of the molnupiravir-1r42 complex revealed a small fluctuation until 8 ns, while from 8 ns to 50 ns, this fluctuation decreased and became stable. The data collected by our study suggests that it is possible for molnupiravir to use multiple ways in averting the infection of SARSCoV-2 (COVID-19).

REFERENCES

[1] Yang, P., Wang, X. COVID-19: a new challenge for human beings, Cellular & Molecular Immunology, 17(5), 555-557, 2020.

[2] Ullrich, S., Nitsche, C. The SARS-CoV-2 main protease as drug target, Bioorganic & Medicinal Chemistry Letters, 30(17), 127377, 2020.

[3] Qiao, J., Li, Y. S., Zeng, R., Liu, F. L., Luo, R. H., Huang, C., Wang, Y. F., Zhang, J., Quan, B., Shen, C., Mao, X., Liu, X., Sun, W., Yang, W., Ni, X., Wang, K., Xu, L., Duan, Z. L., Zou, Q. C., Zhang, H. L., Qu, W., Long, Y. H. P., Li, M. H., Yang, R. C., Liu, X., You, J., Zhou, Y., Yao, R., Li, W. P., Liu, J. M., Chen, P., Liu, Y., Lin, G. F., Yang, X., Zou, J., Li, L., Hu, Y., Lu, G. W., Li, W. M., Wei, Y. Q., Zheng, Y. T., Lei, J., Yang, S. SARS-CoV-2 M^pro inhibitors with antiviral activity in a transgenic mouse model, Science, 371(6536), 1374-1378, 2021.

[4] Benkovics, T., McIntosh, J. A., Silverman, S. M., Kong, J., Maligres, P., Itoh, T., Yang, H., Huffman, M. A., Verma, D., Pan, W., Ho, H., Vroom, J., Knight, A., Hurtak, J., Morris, W., Strotman, N.A., Murphy, G., Maloney, K. M., Fier, P. S. Evolving to an Ideal Synthesis of Molnupiravir, an Investigational Treatment for COVID-19, 2020.

[5] Zarenezhad, E., Marzi, M. Review on molnupiravir as a promising oral drug for the treatment of COVID-19, Medicinal Chemistry Research, 1-12, 2022.

[6] Cox, R. M., Wolf, J. D., Plemper, R. K. Therapeutically administered ribonucleoside analogue MK-4482/EIDD-2801 blocks SARS-CoV-2 transmission in ferrets, Nature microbiology, 6(1), 11-18, 2020.

[7] Painter, G. R., Natchus. M. G., Cohen, O., Holman W., Painter, W. P. Developing a direct acting, orally available antiviral agent in a pandemic: the evolution of molnupiravir as a potential treatment for COVID-19, Current opinion in virology, 50, 17-22, 2021.

[8] Fischer, W., Eron Jr, J. J., Holman, W., Cohen, M. S., Fang, L., Szewczyk, L. J., Sheahan, T. P., Baric, R., Mollan, K. R., Wolfe, C. R., Duke, E. R., Azizad, M. M., Borroto-Esoda, K., Wohl, D. A., Loftis, A. J., Alabanza, P., Lipansky, F., Painter, W. P. Molnupiravir, an Oral Antiviral Treatment for COVID-19, MedRxiv, 2021-06., 2021.

[9] Singh, A. K., Singh, A., Singh, R., Misra, A. An updated practical guideline on use of molnupiravir and comparison with agents having emergency use authorization for treatment of COVID-19, Diabetes & Metabolic Syndrome: Clinical Research & Reviews, 16(2), 102396, 2022.

[10] Painter, W. P., Holman W., Bush J.A., Almazedi F., Malik H., Eraut N. C. J. E., Morin M. J., Szewczyk L. J., Painter G. R. Human Safety, Tolerability, and Pharmacokinetics of a Novel Broad-Spectrum Oral Antiviral Compound, Molnupiravir, with Activity Against SARS-CoV-2, medrxiv, 2020-12., 2020.

[11] Abdel-Maksoud, K., al-Badri, M. A., Lorenz, C., Essex, J. W. Allosteric regulation of SARS-CoV-2 protease: towards informed structure-based drug discovery, 2020.

[12] Baindara, P., Roy, D., Mandal, S. M. Omicron favors neuropilin1 binding over ACE2: Increased infectivity and available drugs, 2022.

[13] Shao, Y., Molnar, L. F., Jung, Y., Kussmann, J., Ochsenfeld, C., Brown, S. T., Gilbert, A. T. B., Slipchenko, L. V., Levchenko, S. V., O'Neill, D. P., DiStasio, R. A., Lochan, R. C., Wang, T., Beran, G. J. O., Besley, N. A., Herbert, J. M., Lin, C. Y., Van Voorhis, T., Chien, S. H., Head Gordon, M. Advances in methods and algorithms in a modern quantum chemistry program package, Physical Chemistry Chemical Physics, 8(27), 3172–3191, 2006.

[14] Dewar, M. J. S., Zoebisch, E. G., Healy, E. F., Stewart, J. J. AM1: A new general purpose quantum mechanical molecular model, Journal of the American Chemical Society, 107(13), 3902–3909, 1985.

[15] Jurcik, A., Bednar, D., Byska, J., Marques, S. M., Furmanova, K., Daniel, L., Kozlikova, B. CAVER Analyst 2.0: analysis and visualization of channels and tunnels in protein structures and molecular dynamics trajectories, Bioinformatics, 34(20), 3586-3588, 2018.

[16] Trott, O., Olson, A. J. AutoDock Vina: improving the speed and accuracy of docking with a new scoring function, efficient optimization, and multithreading, Journal of computational chemistry, 31(2), 455-461, 2010.

[17] Hao, G. F., Jiang, W., Ye, Y. N., Wu, F. X., Zhu, X. L., Guo, F. B., Yang, G. F. ACFIS: a web server for fragment-based drug discovery, Nucleic acids research, 44(W1), W550-W556, 2016.

[18] Hao, G. F., Wang, F., Li, H., Zhu, X. L., Yang, W. C., Huang, L. S., Yang, G. F. Computational discovery of picomolar Q o site inhibitors of cytochrome bc 1 complex, Journal of the American Chemical Society, 134(27), 11168-11176, 2012.

[19] Yang, J. F., Wang, F., Jiang, W., Zhou, G. Y., Li, C. Z., Zhu, X. L., Yang, G. F. PADFrag: a database built for the exploration of bioactive fragment space for drug discovery, Journal of chemical information and modeling, 58(9), 1725-1730, 2018.

[20] Cheron, N., Jasty, N., Shakhnovich, E. I. OpenGrowth: an automated and rational algorithm for finding new protein ligands, Journal of medicinal chemistry, 59(9), 4171-4188, 2016.

[21] Abraham, M. J., Murtola, T., Schulz, R., Pall, S., Smith, J. C., Hess, B., & Lindahl, E. GROMACS: High performance molecular simulations through multi-level parallelism from laptops to supercomputers, SoftwareX, 1–2,19–25, 2015.

[22] Bekker, H., Berendsen, H. J. C., Dijkstra, E. J., Achterop, S., Vondrumen, R., Vanderspoel, D., Sijbers, A., Keegstra, H., Renardus, M. K. R. Gromacs–A parallel computer for molecular-dynamics simulations, In 4th International Conference on Computational Physics (PC 92) (pp. 252–256), World Scientific Publishing, 1993.

[23] Bjelkmar, P., Larsson, P., Cuendet, M. A., Hess, B., Lindahl, E. Implementation of the CHARMM force field in GROMACS: Analysis of protein stability effects from correction maps, virtual interaction sites, and water models, Journal of Chemical Theory and Computation, 6(2), 459–466, 2010.

[24] Lindorff-Larsen, K., Piana, S., Palmo, K., Maragakis, P., Klepeis, J. L., Dror, R. O., Shaw, D. E. Improved side-chain torsion potentials for the Amber ff99SB protein force field, Proteins, 78(8), 1950–1958, 2010.

[25] van Gunsteren, W. F., Billeter, S. R., Eising, A. A., Hünenberger, P. H., Krüger, P. K. H. C., Mark, A. E., Scott, W.R.P., Tironi, I. G. Biomolecular simulation: The GROMOS96 manual and user guide, Vdf Hochschulverlag AG an der ETH Zürich, Zürich, 86,1–1044, 1996.

[26] Daura, X., Mark, A. E., Van Gunsteren, W. F. Parametrization of aliphatic CHn united atoms of GROMOS96 force field, Journal of Computational Chemistry, 19(5), 535–547, 1998.

[27] Gorai, S., Junghare, V., Kundu, K., Gharui, S., Kumar, M., Patro, B. S., Nayak, S. K., Hazra, S., Mula, S. Synthesis of dihydrobenzo furo [3,2-b] chromenes as potential 3CLpro inhibitors of SARS-CoV-2: A molecular docking and molecular dynamics study, ChemMedChem, 17(8), e202100782, 2022.

[28] Kalimuthu, A. K., Panneerselvam, T., Pavadai, P., Pandian, S. R. K., Sundar, K., Murugesan, S., Ammunje, D. N., Kumar, S., Arunachalam, S., Kunjiappan, S. Pharmacoinformatics-based investigation of bio active compounds of Rasam (South Indian recipe) against human cancer, Scientific Reports, 11(1), 21488, 2021.

[29] Oostenbrink, C., Villa, A., Mark, A. E., & Van Gunsteren, W. F. A biomolecular force field based on the free enthalpy of hydration and solvation: The GROMOS force-field parameter sets 53A5 and 53A6, Journal of Computational Chemistry, 25(13), 1656–1676, 2004.

[30] Prasanna, D., Runthala, A., Shantier, S. W. NudF-boosted strategy to improve the yield of DXS pathway, bioRxiv, 2022-03, 2022.

[31] Tumskiy, R. S., Tumskaia, A. V. Multistep rational molecular design and combined docking for discovery of novel classes of inhibitors of SARS-CoV-2 main protease 3CLpro, Chemical Physics Letters, 780, 138894, 2021.

[32] Vishvakarma, V. K., Singh, M. B., Jain, P., Kumari, K., Singh, P. Hunting the main protease of SARS-CoV-2 by plitidepsin: Molecular docking and temperature-dependent molecular dynamics simulations, Amino Acids, 54(2), 205–213, 2022.

[33] Walls, A. C., Park, Y. J., Tortorici, M. A., Wall, A., McGuire, A. T., Veesler, D. Structure, function, and antigenicity of the SARS-CoV-2 spike glycoprotein, Cell, 181(2), 281-292, 2020.

[34] Lan, J., Ge, J., Yu, J., Shan, S., Zhou, H., Fan, S., Wang, X. Structure of the SARS-CoV-2 spike receptor-binding domain bound to the ACE2 receptor, Nature, 581(7807), 215-220, 2020.

[35] Cetin, A., Donmez, A., Dalar, A., Bildirici, I. Amino acid and dicyclohexylurea linked pyrazole analogues: synthesis, in silico and in vitro studies, ChemistrySelect 8, e202204926, 2023.

[36] Zhang, B., Zhao, Y., Jin, Z., Liu, X., Yang, H., Rao, Z. The Crystal Structure of COVID-19 Main Protease in Apo Form, Publ. Online, 2020.

[37] Jin, Z., Du, X., Xu, Y., Deng, Y., Liu, M., Zhao, Y., Zhang, B., Li, X., Zhang, L., Peng, C., Duan, Y., et al. Structure of Mpro from SARS-CoV-2 and discovery of its inhibitors, Nature, 582, 289-293, 2020.

[38] Mahdian, S., Zarrabi, M., Panahi, Y., Dabbagh, S. Repurposing FDA-approved drugs to fight COVID-19 using in silico methods: targeting SARS-CoV-2 RdRp enzyme and host cell receptors (ACE2, CD147) through virtual screening and molecular dynamic simulations, Informatics in medicine unlocked, 23, 100541, 2021.

[39] Rahman, M. R., Banik, A., Chowdhury, I. M., Sajib, E. H., Sarkar, S. Identification of potential antivirals against SARS-CoV-2 using virtual screening method, Informatics in medicine unlocked, 23, 100531, 2021.

[40] Celik, S., Akyuz, S., Ozel, A. E. Vibrational spectroscopic characterization and structural investigations of Cepharanthine, a natural alkaloid, Journal of Molecular Structure, 1258, 132693, 2022.

[41] Sagaama, A., Brandan, S. A., Issa, T. B., Issaoui, N. Searching potential antiviral candidates for the treatment of the 2019 novel coronavirus based on DFT calculations and molecular docking, Heliyon, 6(8), e04640, 2020.

[42] Cetin, A. Some flavolignans as potent Sars-Cov-2 inhibitors via molecular docking, molecular dynamic simulations and ADME analysis. Current Computer-Aided Drug Design, 18(5), 337-346, 2022.

[43] Romeo, A., Iacovelli, F., Falconi, M. Fighting Sars-Cov-2 using natural compounds: a virtual screening analysis, High Performance Computing on CRESCO Infrastructure: research activity and results 2020, 159, 2021.

[44] Srivastava, A., Siddiqui, S., Ahmad, R., Mehrotra, S., Ahmad, B., Srivastava, A. N. Exploring nature's bounty: identification of Withania somnifera as a promising source of therapeutic agents against COVID-19 by virtual screening and in silico evaluation, Journal of Biomolecular Structure and Dynamics, 40(4), 1858-1908, 2022.

[45] Khan, N., Fazal, S., Malik, R. M., Azam, S., Jan, S. A., Kanwal, A., Jan, S. A. N-silico analysis of turmeric as an anti-inflammatory agent against ace2 receptor, Pak. J. Bot., 55(2): 763-778, 2023.

[46] Quang, N. M., Linh, B. T. T., Uyen, T. T., Ngoc, V. T. B., Hoa, T. T., Van Tat, P. Discovery of novel thiazole derivatives as anti-breast cancer agents (MCF-7) and validation of homologous effects on SARS-CoV-2 virus using in silico approaches, Vietnam Journal of Chemistry, 61, 17-29, 2023.

[47] Mohan, M., Rekha, P., Gokulraj, P., Samy, P. A., Thirumalaisamy, R., Khan, R., Aroulmoji, V. Molecular Studies of Antiviral Drug Atazanavir and Hyaluronic Acid-Atazanavir conjugate as Novel Drugs to Target SARS-CoV-2 Viral Proteins, International journal of advanced Science and Engineering, 10(3), 3581-3592, 2024.